ACADEMIC PRESS

Available online at www.sciencedirect.com
SCIENCE DIRECT®

VIROLOGY

Virology 306 (2003) 147–161

www.elsevier.com/locate/yviro

Human immunodeficiency virus type-1 integrase containing a glycine to serine mutation at position 140 is attenuated for catalysis and resistant to integrase inhibitors

Peter J. King,[a,1] Deborah J. Lee,[a] Ryan A. Reinke,[a] Joseph G. Victoria,[a] Keola Beale,[c] and W. Edward Robinson, Jr.[a,b,*]

[a] *Departments of Microbiology and Molecular Genetics, University of California, Irvine, CA 92697, USA*
[b] *Department of Medicine, University of California, Irvine, CA 92697, USA*
[c] *Department of Pathology, University of California, Irvine, CA 92697-4800, USA*

Received 11 July 2002; returned to author for revision 12 September 2002; accepted 20 September 2002

Abstract

L-chicoric acid (L-CA) is a potent inhibitor of HIV integrase (IN) in vitro. In this report, the effects of a glycine to serine mutation at position 140 (G140S) on HIV IN and its effects on IN inhibitor resistance are described. HIV containing the G140S mutation showed a delay in replication. Using real-time polymerase chain reaction, the delay was secondary to a failure in integration. The mutant protein (IN_{G140S}) was attenuated approximately four-fold for catalysis under equilibrium conditions compared to wild-type IN (IN_{WT}) and attenuated five-fold in steady-state kinetic analysis of disintegration. Fifty percent inhibitory concentration assays were performed with IN inhibitors against both IN proteins in disintegration and strand transfer reactions. IN_{G140S} was resistant to both L-CA and L-731,988, a diketoacid. HIV containing the mutation was resistant to both inhibitors as well. The G140S mutation attenuates IN activity and confers resistance to IN inhibitors, suggesting that diketoacids and L-CA interact with a similar binding site on HIV IN.

Keywords: Real-Time polymerase chain reaction; Integration; Experimental antiviral agents; Acquired immune deficiency syndrome; Kinetics; Biochemistry; Drug resistance; HIV replication

Introduction

Integration, catalyzed by the viral enzyme integrase (IN), is a required step in the life cycle of the human immunodeficiency virus (HIV) (Sakai et al., 1993). Mutation of critical residues within IN results in non-productive infections characterized by short-term, low-level expression of some viral proteins (Stevenson et al., 1990), a failure to produce progeny virions (LaFemina et al., 1992; Sakai et al., 1993), and the eventual circularization and degradation of reverse-transcribed viral cDNA (Wiskerchen and Muesing, 1995). A relatively small number of potent inhibitors of IN in vitro have been described to date and few have possessed antiviral activity at non-toxic concentrations in cell culture (reviewed in Pommier and Neamati, 1999; Robinson, 1998).

IN is comprised of three separately folded functional domains as determined by structural, complementation, and mutational analyses (Reviewed in Andrake and Skalka, 1996; Rice et al., 1996). The central catalytic core domain of HIV IN contains three amino acid residues, Asp_{64}, Asp_{116}, and Glu_{152}, in a spatial arrangement of $DX_{39-58}DX_{35}E$, which is invariant for retroviral IN's, as well as IN's of yeast retrotransposons and some bacterial transposases (Kulkosky et al., 1992). These residues coordinate an absolutely required divalent metal cation (Mn^{2+}

* Corresponding author. Department of Pathology, D440 Med Sci I, University of California, Irvine, CA 92697-4800. Fax: +949-824-2505.
E-mail address: ewrobins@uci.edu (W.E. Robinson).
[1] Current address: Department of Biology, Stephen F. Austin State University, Nacogdoches, TX.

0042-6822/03/$ – see front matter © 2003 Elsevier Science (USA). All rights reserved.
PII: S0042-6822(02)00042-9

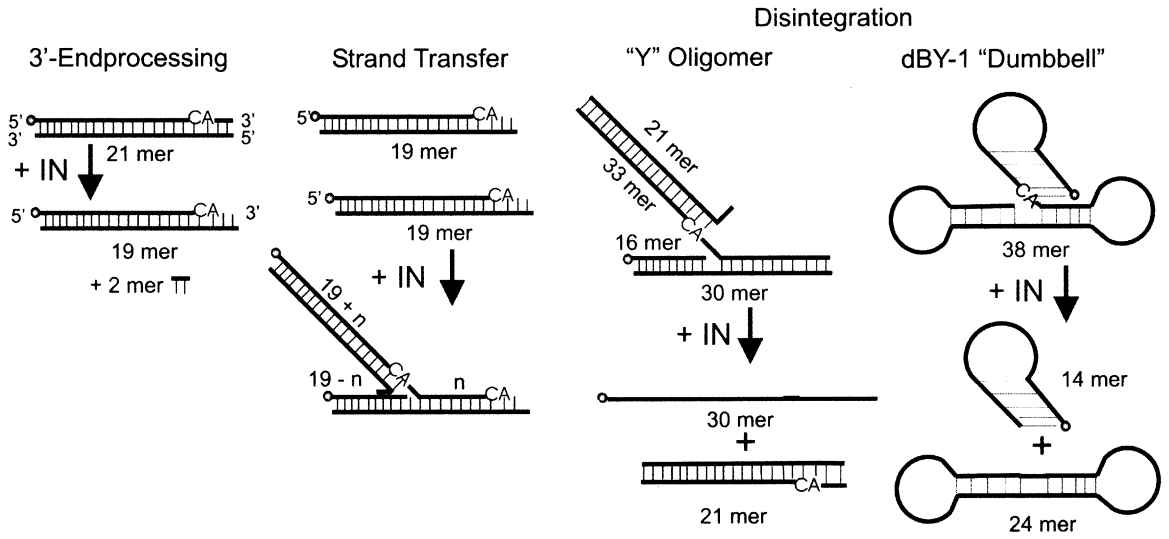

Fig. 1. Oligonucleotide substrates for in vitro IN assays. Oligonucleotide substrates for the 3′ end processing/ strand transfer assay are complementary, 21 nucleotide oligomers with sequences derived from the U5 region of the HIV-1 LTR (V1/V2). Substrates for strand transfer alone are complementary 19 and 21 nucleotide oligomers representing end processed LTR DNA. Substrates for the disintegration assay are comprised of either four complementary oligomers (Y oligomer substrate) or a single self-complementary oligonucleotide (db-Y1, dumbbell oligomer). Substrates were 5′ end-labeled with γ^{32}P-dATP and experiments performed with recombinant HIV IN in vitro as previously described (Chow, 1997).

or Mg^{2+}) (Bujacz et al., 1996a; Bujacz et al., 1996b; Goldgur et al., 1998). The sequences of the amino- and carboxyl-terminal domains of IN are less conserved (Johnson et al., 1986).

As a first step for integration, IN removes the two terminal nucleotides from the 3′ end of each LTR. This endonucleolytic cleavage, termed 3′ end processing, occurs adjacent to a highly conserved CpA dinucleotide located at each viral 3′ end (Brown et al., 1989; Fujiwara and Mizuuchi, 1988; Roth et al., 1989). The processed viral DNA ends are then covalently inserted into the DNA of the infected cell by a concerted cleavage-ligation reaction termed strand transfer (Brown et al., 1989; Fujiwara and Mizuuchi, 1988). Integration is likely completed by the actions of the host cell DNA repair machinery (Miller, et al., 1995), thus producing a stable, integrated provirus.

The in vivo activities of IN can be measured in vitro by utilizing purified recombinant IN as well as ^{32}P end-labeled oligonucleotide substrates with sequences derived from the HIV LTR (Bushman and Craigie, 1991; Chow, 1997; Chow and Brown, 1994b; Chow et al., 1992) (Fig. 1). Oligonucleotide assays of both 3′ end processing and strand transfer have been utilized to demonstrate the requirements for integration (Bushman and Craigie, 1991; Sherman et al., 1992; Sherman and Fyfe, 1990). The reversal of integration, termed disintegration, can be measured utilizing both Y-shaped and dumbbell -shaped oligonucleotide substrates (Chow, 1997) (Fig. 1). All four substrates have been used to identify inhibitors of IN, while the disintegration substrate has been useful in separating inhibition of the catalytic activities of IN from inhibition of other IN activities such as DNA binding (Robinson et al., 1996a).

L-chicoric acid (L-CA) (see Structures) is a potent inhibitor of IN in vitro (Robinson et al., 1996a; Robinson et al., 1996b), which also inhibits viral replication at non-toxic concentrations (Robinson et al., 1996a; Robinson et al.,

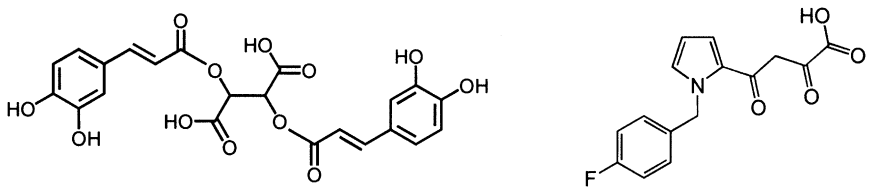

L-Chicoric Acid L-731,988

Structures

1996b). Intracellular inhibition of IN was demonstrated through selection of an L-CA-resistant variant of HIV and the subsequent isolation of a mutant virus containing a mutation within IN, glycine 140 to serine (IN_{G140S}). This mutation was sufficient to confer L-CA-resistance to otherwise wild-type HIV, as demonstrated through sub-allelic reconstruction of the mutant virus (King and Robinson, 1998). A recent report suggests that L-CA also blocks HIV entry (Pluymers et al., 2000). L-CA belongs to a family of compounds having a central carboxylated core and two catechol rings. This group, the dicaffeoyltartaric acids, are selective inhibitors of IN and do not inhibit the activity of structurally-related metalloenzymes (McDougall et al., 1998; Zhu et al., 1999). Recent molecular modeling predictions (Sotriffer et al., 2000), based on the crystal structure of an IN-inhibitor complex (Goldgur et al., 1999), have suggested that L-CA fits into a drug binding pocket and fills the entire catalytic groove of HIV IN.

The diketoacids are structurally distinct from L-CA and its analogues yet share certain similarities, including a free carboxylic acid and an adjacent carbonyl group (see Structures), which are required for activity (Hazuda et al., 2000; King et al., 1999; Reinke et al., 2002). The similarity in chemical constituents necessary for activity led to the hypothesis that L-CA and the diketoacids fill the same binding pocket. However, the diketoacids inhibit only strand transfer (Espeseth et al., 2000; Hazuda et al., 2000), not 3′ end processing or disintegration, suggesting that they fit into the drug binding pocket differently than L-CA.

The mechanism by which the IN_{G140S} mutation confers resistance to L-CA has not been established. Additionally, the effects of this mutation on viral integration and on IN catalytic activity at the biochemical level have not been examined previously. This report describes the effects of the IN_{G140S} on viral replication and IN activity in vitro. Furthermore, the effects of the G140S mutation on the susceptibility of HIV to several anti-HIV agents, including L-731,988 (Hazuda et al., 2000), a diketoacid, were studied to determine whether resistance to L-CA and L-731,988 map to the same amino acid.

Results

HIV containing the IN G140S mutation is mildly attenuated for replication

HIV containing the single amino acid change at glycine 140 of IN, $HIV_{NL4-3:ING140S}$, is resistant to L-CA in vitro and replicates slower than wild-type HIV_{NL4-3} (King and Robinson, 1998). $HIV_{NL4-3:ING140S}$ replication in MT-2 cells was compared to reference HIV_{NL4-3} at equal reverse transcriptase (RT) activity or equal fifty percent tissue culture infectious dose ($TCID_{50}$). Viral replication was quantitated by RT release into the culture supernatant and by immunofluorescence assay (IFA) (Fig. 2). $HIV_{NL4-3:ING140S}$ displayed a slight delay in the time to infect 100% of MT-2 cells. This was almost entirely due to a delay in detection of the virus during the first 36 h post inoculation. Delay was not secondary to different amounts of input virus, as the same delay was seen whether equal amounts of input RT (10,000 cpm) or infectious virions (20,000 $TCID_{50}$) were used. As described previously, both HIV_{NL4-3} and $HIV_{NL4-3:ING140S}$ were generated by sub-allelic reconstruction and contained the silent mutations used to clone the IN genes (King and Robinson, 1998).

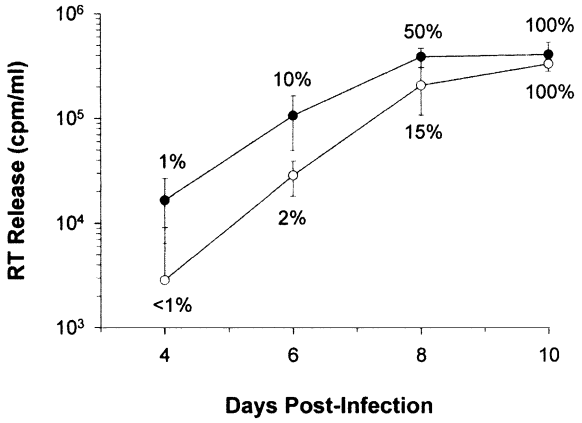

Fig. 2. Viral replication kinetics of HIV_{NL4-3} versus $HIV_{NL4-3:ING140S}$. MT-2 cells were infected with either HIV_{NL4-3} (●), or $HIV_{NL4-3:ING140S}$ (○). Cultures were monitored for antigen production by IFA and virus-associated RT activity every other day post infection (Robinson et al., 1996b). Data points represent mean values of triplicate infections from three experiments. Error bars represent one standard deviation. The percentages of HIV antigen positive cells at each time point post-infection are indicated at each data point. Data shown is for infection with equal levels of virus-associated RT activity. Similar results were obtained when equal amounts of infectious particles for each virus were used (data not shown).

The delay in replication appeared to be in the initial hours post infection, as the slope of the growth curve for the two viruses was the same or steeper for $HIV_{NL4-3:ING140S}$. These data suggested that a reversion or compensatory mutation might have occurred. Virus was pelleted from MT-2 cells when the culture was 100% positive for HIV antigens after two different inocula of the $HIV_{NL4-3:ING140S}$. Both inocula displayed a similar 12–18 h delay in the time to infect 100% of the MT-2 cells. The virions were lysed and the IN gene was amplified using reverse transcriptase polymerase chain reaction (RT-PCR). The IN genes from four clones, two from each culture, were sequenced and no mutations within IN were noted in any of the four clones. These data are consistent with those obtained from multiple experiments in which $HIV_{NL4-3:ING140S}$ remains stable in H9 cells (King and Robinson, 1998, and data not shown).

Quantitative real-time polymerase chain reaction (PCR) indicates a defect in integration

Equal amounts of HIV_{NL4-3} and $HIV_{NL4-3:ING140S}$ by RT activity were inoculated onto H9 cells and the levels of

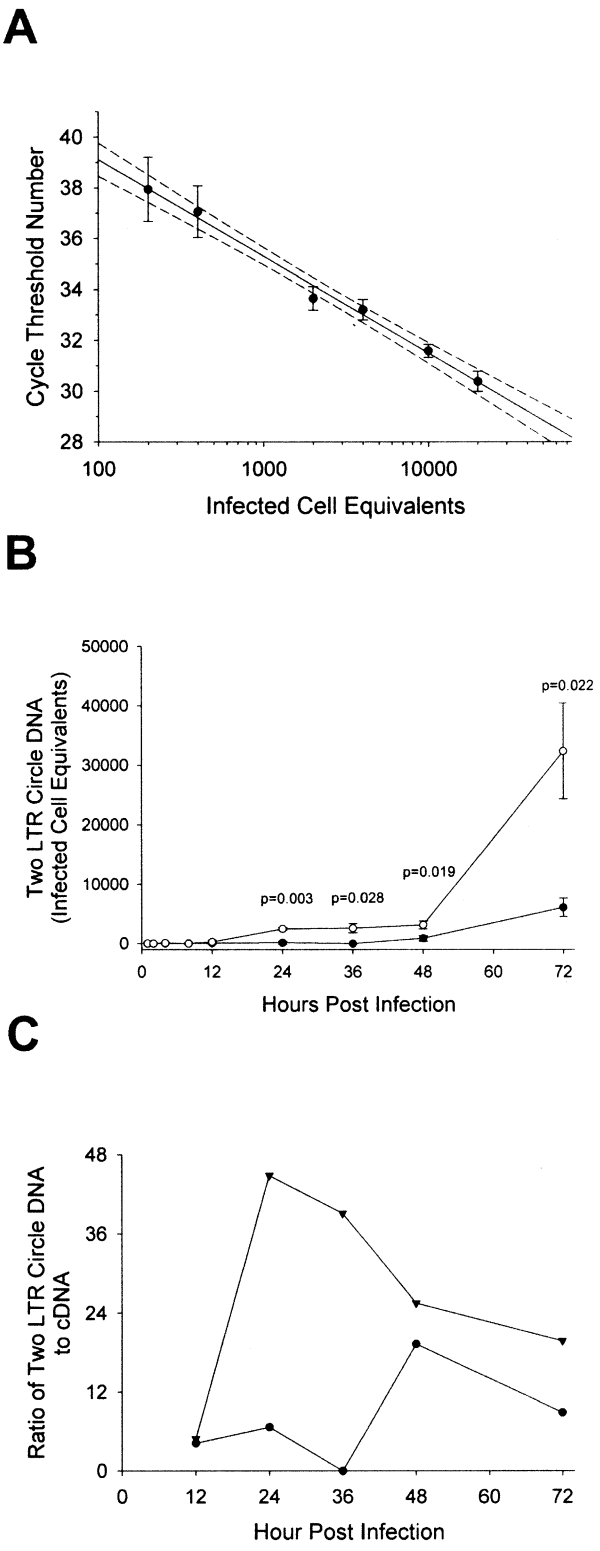

Fig. 3. Ratio of two LTR circle DNA to cDNA by real-time PCR. Equal amounts of $HIV_{NL4-3:INWT}$ versus $HIV_{NL4-3:ING140S}$, as measured by RT assay, were inoculated in triplicate onto H9 cells at a multiplicity of infection of less than 1. 1×10^6 H9 cells were lysed at timepoints from 1 to 72 h p.i. The amounts of cDNA as measured by the M661/M667 primer pair (Zack et al., 1990) and SYBR-I green dye and the relative levels of two LTR circle DNA as measured by MH535/MH536 primer pair (Butler et al., 2001) and SYBR-I green dye were determined. A) Standard curve from six replicates used to calculate the levels of two LTR circle DNA. Diluting cell lysate from 20,000-0 HIV_{LAI} chronically-infected H9 cells into the lysate of 0–20,000 H9 cells generated the standard curve. The infected cell equivalents for each curve were 20, 40, 200, 400, 2000, 4000, and 20,000 infected cells in the DNA from a total of 20,000 H9 cells. Solid line is linear regression analysis ($r^2 = 0.992$); the dashed lines are the 95% confidence intervals. B) The levels of two LTR circle DNA at each timepoint in infected cell equivalents. Closed circles, HIV_{NL4-3}; open circles, $HIV_{NL4-3:ING140S}$. Points are the means of triplicate infections; the error bars are one standard deviation. Statistical significance, if less than 0.05, is illustrated above each point and was determined by Student's *t* test assuming equal variances. C) To control for different levels of cDNA, the ratio of two LTR circle DNA to cDNA was determined at each timepoint. Ratios were calculated using the mean cDNA and mean two LTR circle DNA levels calculated from triplicate infections. Closed circles, HIV_{NL4-3}; closed triangles, $HIV_{NL4-3:ING140S}$.

cDNA and two LTR circle DNA were quantified by real-time PCR. In Fig. 3A, the standard curve used to calculate two LTR circle DNA is shown. The results are highly linear ($r^2 = 0.992$). In Fig. 3B, the total two LTR circle DNA in infected cell equivalents for each virus is shown. There was a statistically significant increase in two LTR circle DNA at all timepoints after 12 h p.i. in the $HIV_{NL4-3:ING140S}$ compared to the control virus, HIV_{NL4-3} ($p < 0.03$). Figure 3C illustrates the mean ratio of two LTR circle DNA to cDNA from triplicate infections. $HIV_{NL4-3:ING140S}$ shows a higher ratio of two LTR circle DNA to cDNA when compared to HIV_{NL4-3}, consistent with a failure in integration for $HIV_{NL4-3:ING140S}$. Nuclear entry is unaffected by the mutation as two LTR circle formation occurs within the nucleus (reviewed in Brown, 1997). Reverse transcription was unaffected, as the kinetics of reverse transcription, as measured using real-time PCR and primers for early (AA55/M667) and late (M661/M667) DNA products (Zack et al., 1990), were the same for both viruses over the first 24 h of infection (data not shown).

$HIV_{NL4-3:ING140S}$ is resistant to multiple IN inhibitors

$HIV_{NL4-3:ING140S}$ had been shown previously to be resistant to L-CA: $HIV_{NL4-3:ING140S}$ was inhibited by L-CA no more than 30% at any concentration (King and Robinson, 1998). When $HIV_{NL4-3:ING140S}$ was replicated in the presence of zidovudine, an RT inhibitor, both $HIV_{NL4-3:ING140S}$ and HIV_{NL4-3} showed equal susceptibility (Fig. 4A), having fifty percent effective concentrations (EC_{50}) of approximately 20–40 nM. However, when the virus was replicated in the presence of L-731,988, no EC_{50} was obtained (Fig. 4B). Indeed, there was some anti-HIV activity of L-731,988 but it plateaued at approximately 35% protection, nearly identical to the results observed for L-CA (King and Robinson, 1998). Furthermore, $HIV_{NL4-3:ING140S}$ and HIV_{NL4-3} were equally susceptible to other RT and protease inhibitors (Fig. 5). Therefore, the IN_{G140S} mutation confers resistance to both L-CA and L-731,988 but has no effect on the susceptibility of the virus to inhibitors that act on other HIV enzymes (Fig. 5).

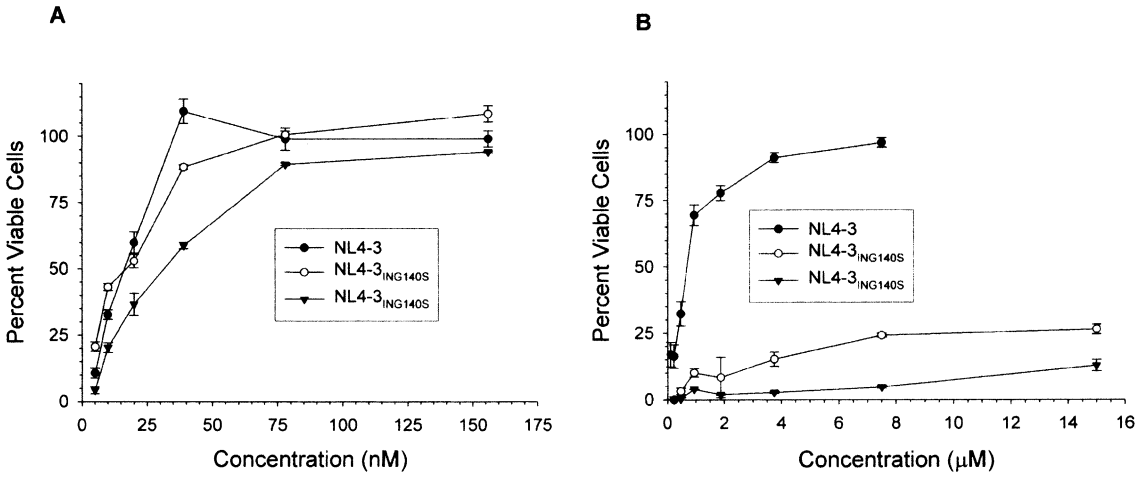

Fig. 4. $HIV_{NL4-3:ING140S}$ is resistant to L-731,988 but not zidovudine. Either HIV_{NL4-3} or $HIV_{NL4-3:ING140S}$, was preincubated with H_2O (virus control; 0% viable) or varying concentrations of Panel A: zidovudine, or Panel B: L-731,988 for 1 h. Next, MT-2 cells were added and the virus and cells incubated for four days before harvesting the cells to quantify HIV-induced cytopathic effect. Cells incubated in the absence of HIV were 100% viable. For both panels each point is the mean of triplicate infections and error bars are one standard deviation. Susceptibilities of HIV_{NL4-3} from one experiment and $HIV_{NL4-3:ING140S}$ from two experiments are given. Each experiment represents triplicate infections for a total of six separate infections. Anti-HIV assays were performed essentially as described previously (King and Robinson, 1998). These results are consistent with those previously published for HIV_{NL4-3} and $HIV_{NL4-3:ING140S}$ in the presence of zivodudine and L-CA (King and Robinson, 1998).

Purified IN_{G140S} is attenuated for catalytic activity

IN_{WT} and IN_{G140S} proteins were expressed and isolated at greater than 90% purity as analyzed by SDS–PAGE and Coomassie blue staining (data not shown). Purified IN proteins were used at equal concentrations in the disintegration assay. At each protein concentration tested, IN_{G140S} was attenuated for disintegration activity compared to IN_{WT} (Figs. 6A and 6B). Linear regression analysis, using molecular activity data points for both proteins that were within the linear range of measurement (IN_{WT} $r^2 = 0.98$, IN_{G140S} $r^2 = 0.98$), demonstrated an approximately eight-fold reduction in disintegration activity of IN_{G140S} compared to IN_{WT}. Similar attenuation of IN_{G140S} for 3′ end processing, when compared to IN_{WT}, was also observed (Figs. 7A and 7B).

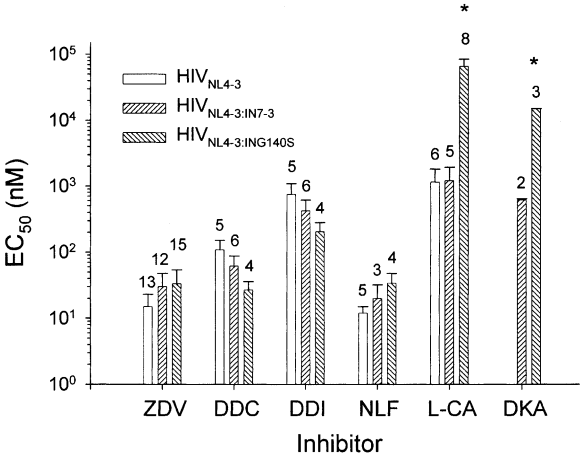

Fig. 5. $HIV_{NL4-3:ING140S}$ is resistant to IN inhibitors but not to RT or PR inhibitors. Each virus was inoculated onto MT-2 cells in triplicate wells of a 96 well plate in the presence of increasing concentrations of the indicated anti-HIV compound. Cells were harvested and stained to determine protection from the lytic effects of HIV as described previously. Numbers above each column are the number of replicate experiments used to calculate the mean EC_{50}. The actual number of infections is three times that number. An asterisk represents a statistically significant difference in IC_{50}. Error bars are 1 SD. ZDV = zidovudine; DDC = dideoxycytidine; DDI = dideoxyinosine; NLF = nelfinavir; L-CA = L-chicoric acid; DKA = L-731,988. $HIV_{NL4-3:IN7-3}$ is HIV_{NL4-3} with mutations for IN cloning.

To further analyze the mechanism of IN_{G140S} attenuation, steady-state kinetic analyses of the disintegration reaction were utilized. Amounts of IN_{WT} and IN_{G140S} proteins that gave similar levels of disintegration activity, approximately 40% conversion of disintegration substrate to product in 1 h at 37°C, were incubated with increasing concentrations of disintegration substrate, in excess of enzyme, and the reaction progress measured at four, eight, and twelve minutes (Figs. 8A and 8B). Reactions were performed at least in triplicate with each reaction quantitated from duplicate runs for a total of at least six replicates per data point. Linear regression analysis was performed using data points from each replicate on the Lineweaver-Burk plot (Fig. 8C) to derive the mean V_{max} and K_m for each protein. IN_{WT} (35 nM) displayed a K_m for disintegration substrate of 155 nM. The V_{max} for disintegration catalyzed by IN_{WT} was 3.5×10^{-3} pmol product per pmol IN per minute. Marked enzymatic attenuation was observed when IN_{G140S} at 229 nM was utilized. While the K_m of IN_{G140S} for disintegration substrate (124 nM) was not statistically different than wild-type IN ($P = 0.461$), the V_{max} of IN_{G140S} catalyzed disintegration was approximately five-fold lower (7.4×10^{-4} pmol disintegration product per pmol IN per minute). This

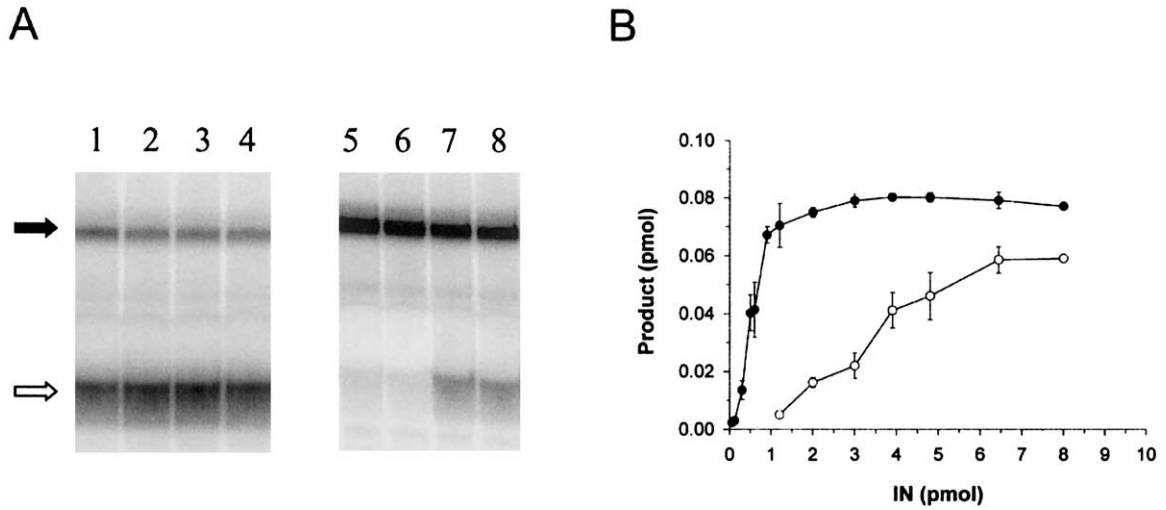

Fig. 6. Molecular activity analysis of the disintegration reaction. Increasing concentrations of IN_{WT} and IN_{G140S} were incubated with 5 nM dumbbell disintegration substrate (db-Y1) for 1 h at 37°C in duplicate. Panel A: Reactions were resolved by 15% denaturing PAGE. Lanes 1 and 2: 195 nM IN_{WT}; lanes 3 and 4:240 nM IN_{WT}; lanes 5 and 6: 195 nM IN_{G140S}; lanes 7 and 8: 240 nM IN_{G140S}. The closed arrow indicates substrate (db-Y1) and the open arrow indicates disintegration product. Panel B: Quantification of data from molecular activity experiments. Closed circles represent IN_{WT} and open circles represent IN_{G140S}. Data points are the means of at least duplicate experiments. Error bars are one standard deviation.

difference was statistically significant ($P < 0.00001$) and is also readily apparent on a Michealis-Menten plot (Fig. 8D).

Biochemical characterization of IN_{G140S}

In an attempt to determine the nature of the IN_{G140S} enzymatic defect, optimal temperature and divalent metal ion concentrations for both proteins were determined. Concentrations of mutant and wildtype IN proteins that gave similar levels of disintegration activity (IN_{WT} = 35 nM, IN_{G140S} = 229 nM) were utilized for these experiments. For IN_{WT} and IN_{G140S} proteins, optimal disintegration activity was observed at 30°C (not shown). Both IN_{WT} and IN_{G140S} displayed the same preference for Mn^{2+} over Mg^{2+} in the disintegration assay with less efficient catalysis in the presence of Mg^{2+} (not shown). Additionally, both wildtype and mutant IN proteins displayed nearly identical concentration profiles for both Mn^{2+} and Mg^{2+} and were inactive with Zn^{2+} (not shown).

To determine whether the IN_{G140S} enzymatic defect resulted from a defect in binding to DNA, equal concentrations of IN_{WT} and IN_{G140S}, or a non-specific protein, hen egg lysozyme (HEL), were incubated with radiolabeled 3′ end processing substrate, followed by filtration of the mixture through a 0.45 μm nitrocellulose filter. IN_{WT} and

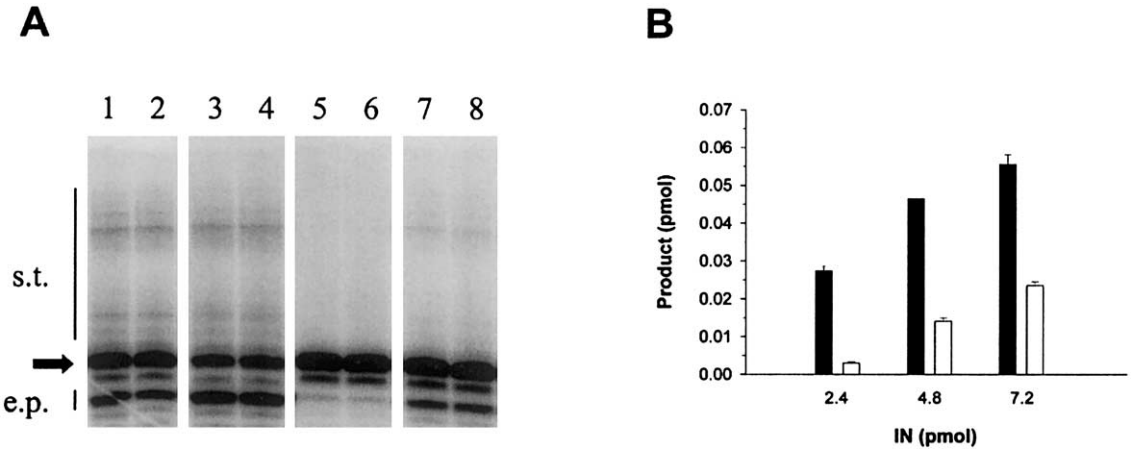

Fig. 7. Molecular activity analysis of the 3′ end processing and strand transfer reactions. Increasing concentrations of IN_{WT} and IN_{G140S} were incubated with 5 nM end processing/strand transfer substrate (V1/V2) for 1 h at 37°C. Panel A: Reactions were resolved by 15% denaturing PAGE. Lanes 1 and 2: 120 nM IN_{WT}; lanes 3 and 4: 360 nM IN_{WT}; lanes 5 and 6: 120 nM IN_{G140S}; lanes 7 and 8: 360 nM IN_{G140S}. The closed arrow indicates the substrate (db-Y1); s.t. indicates the position of strand transfer products; e.p. indicates the position of the band corresponding to end-processed product. Panel B: Quantification of end processing products. Closed bars represent IN_{WT} and open bars represent IN_{G140S}. Data points are the means of at least duplicate experiments. Error bars are one standard deviation.

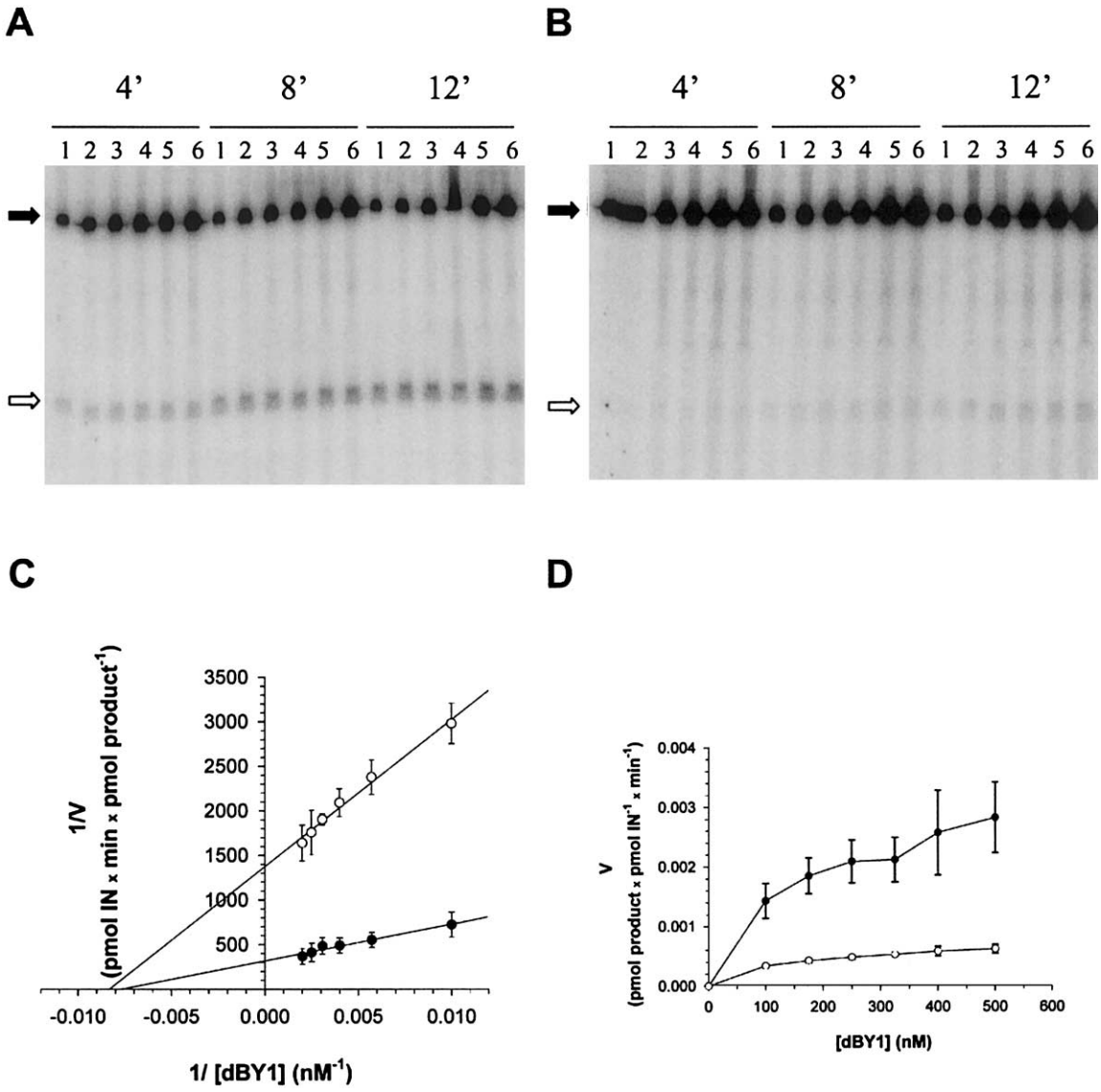

Fig. 8. Steady-state kinetic analysis of the disintegration reaction. IN_{WT} at 35 nM or IN_{G140S} at 229 nM (similar activity levels) were incubated with increasing concentrations of db-Y1. The initial velocity of the reaction at each substrate concentration was determined by measuring the amount of product produced at 4, 8, and 12 minutes and a rate for each reaction was calculated. Panel A: Representative gel for IN_{WT} reactions. Panel B: Representative gel for IN_{G140S} reactions. For Panels A and B, lane 1: 100 nM db-Y1; lane 2: 175 nM db-Y1; lane 3: 250 nM db-Y1; lane 4: 325 nM db-Y1; lane 5: 400 nM db-Y1; lane 6: 500 nM db-Y1. The closed arrow indicates substrate (db-Y1) and the open arrow indicates disintegration product. Time points for each reaction are indicated above each gel. Panel C: Lineweaver-Burk plot for disintegration activities. Linear regression analysis (IN_{WT} $r^2 = 0.96$, IN_{G140S} $r^2 = 0.99$) was utilized to determine V_{max} and K_m for both proteins. Closed circles represent IN_{WT} and open circles represent IN_{G140S}. Data points are means of triplicate experiments, each quantitated from duplicate runs. Error bars are one standard deviation. Panel D: Michealis-Menten plot of the data illustrated in Panel C.

IN_{G140S} bound similar levels of DNA at equal protein concentrations, whereas HEL possessed much lower levels of non-specific DNA binding (Fig. 9). Lower concentrations of IN protein could not be used due to variability in non-specific binding to membranes (data not shown).

IN_{G140S} is resistant to inhibition by IN inhibitors

We measured the sensitivity of IN_{WT} and IN_{G140S} to L-CA and L-731,988 using IC_{50} analysis. For susceptibility to L-CA, the disintegration assay was performed with both proteins at equal levels of disintegration activity, in the presence of increasing concentrations of L-CA, and the level of inhibition using the Y -oligomer substrate at each L-CA concentration was assessed. Triplicate reactions were performed for each protein; each reaction was performed using three replicates. As shown in Table 1, for each of the nine replicates, IN_{G140S} disintegration activity was less sensitive to inhibition by L-CA than IN_{WT}. Indeed, the mean IC_{50} of L-CA against IN_{G140S} was nearly five-fold higher than against IN_{WT} (82 nM vs 372 nM, respectively). This difference was statistically significant ($P < 0.0001$). Similar

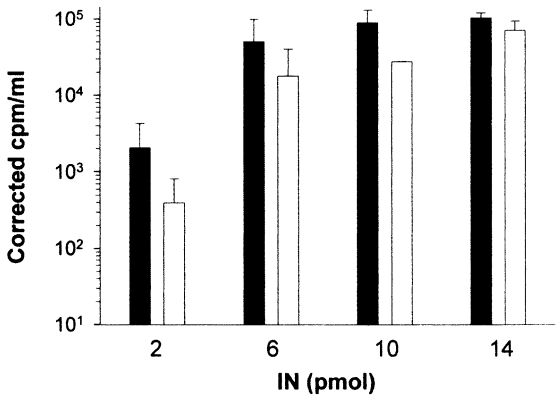

Fig. 9. HIV LTR DNA-binding by IN proteins. Equal concentrations of IN_{WT} (filled bars), IN_{G140S} (open bars), or HEL were incubated with ^{32}P-5′-end-labeled V1/V2 substrate as described (Chow, 1997). Following incubation the mixture was filtered through 0.45 μm nitrocellulose filters, extensively washed, and the filters dried. The extent of IN DNA binding was quantitated by scintillation counting in the presence of liquid scintillant. Bars are means of triplicate experiments with background binding of DNA to HEL subtracted. Error bars are one standard deviation.

results were obtained when IN_{WT} and IN_{G140S} proteins were present in IC_{50} assays at equal protein concentrations (not shown).

Because L-731,988 only inhibits strand transfer, IC_{50} analyses of IN_{WT} and IN_{G140S} in the strand transfer reaction were performed in the presence of L-731,988. As shown in Figure 10, IN_{G140S} was resistant to the anti-IN effects of L-731,988. The IC_{50} of L-731,988 against the two proteins were: IN_{WT} = 825 nM; IN_{G140S} = 3,009 nM (P = 0.01). This four-fold resistance is especially apparent at the highest concentrations of L-731,988 (Lanes 1–9), as the amount of strand transfer product in panels A and B are nearly equal despite five-fold less strand transfer product for IN_{G140S} compared to IN_{WT} in the enzyme control lanes (Enz.). The results for these two reactions are quantified and illustrated in Fig. 10C and the mean of all reactions quantified and shown in Fig. 10D. Therefore, the IN_{G140S} mutation confers cross resistance between L-CA and L-731,988 of 4–5 fold when compared to the reference protein. However, since the G140S mutation severely attenuates the enzymatic activity of the protein, it cannot be ruled out that the effect of the G140S mutation on catalysis alone confers resistance to both inhibitors.

Discussion

Mutation of critical residues of HIV IN results in attenuation of enzymatic function in vitro (Engelman and Craigie, 1992; Leavitt et al., 1993) and viral replication in tissue culture (Engelman et al., 1997; Taddeo et al., 1994). There is often a lack of correlation between enzymatic attenuation observed for mutant IN in vitro and the rate of replication for mutant viruses. We have examined the effects of a previously isolated drug-resistance mutation, IN_{G140S}, on viral replication, enzymatic activity, and drug-resistance. IN_{G140S}, in the context of otherwise wild-type HIV, shows a slight delay in replication compared to wild-type virus (Fig. 2). However, when examining the effect of this mutation on disintegration (Fig. 6) or end processing and strand transfer (Fig. 7) activities of purified recombinant IN under equilibrium conditions, a more dramatic effect was observed. More importantly, these enzymatic defects confer a defect in integration as measured by an increase in the ratio of two LTR circles to cDNA in infected cells (Fig. 3). Surprisingly, despite the effects of the mutation on integration, to date there has been no evidence that reversion mutations occur in either MT-2 or H9 cells. However, compensatory mutations in other viral genes may occur.

To further characterize the enzymatic attenuation afforded by the G140S mutation, as observed under equilibrium conditions, steady-state kinetic analysis was performed with mutant and wild-type IN proteins (Fig. 8).

Table 1
IC_{50} of L-CA against IN_{WT} and ING_{140S}[a]

Experiment Number	IN_{WT}			IN_{G140S}		
	Replicate A	Replicate B	Replicate C	Replicate A	Replicate B	Replicate C
1	70[b]	62	79	340	285	287
2	108	89	99	633	423	633
3	72	79	78	170	260	313
	Mean = 82 nM[c]; SD = 15 nM			Mean = 372 nM[c]; SD = 163 nM		

[a] IN_{WT} or IN_{G140S} was incubated with the "Y"-oligomer disintegration substrate in the presence of increasing concentrations of L-CA for one hour at 37°C as described (King et al., 1999). Following 15% denaturing PAGE, the amount of disintegration substrate produced under each condition was determined by PhosphorImager analysis. IC_{50} were calculated utilizing the CalcuSyn for Windows software package (BioSoft). Data shown are for experiments where IN_{WT} and IN_{G140S} were present at levels that gave similar levels of disintegration activity (IN_{WT} = 25 nM, IN_{G140S} = 195 nM). Similar results were obtained when equal protein concentrations were utilized (data not shown).

[b] IC_{50} in nM.

[c] $P < 0.0001$.

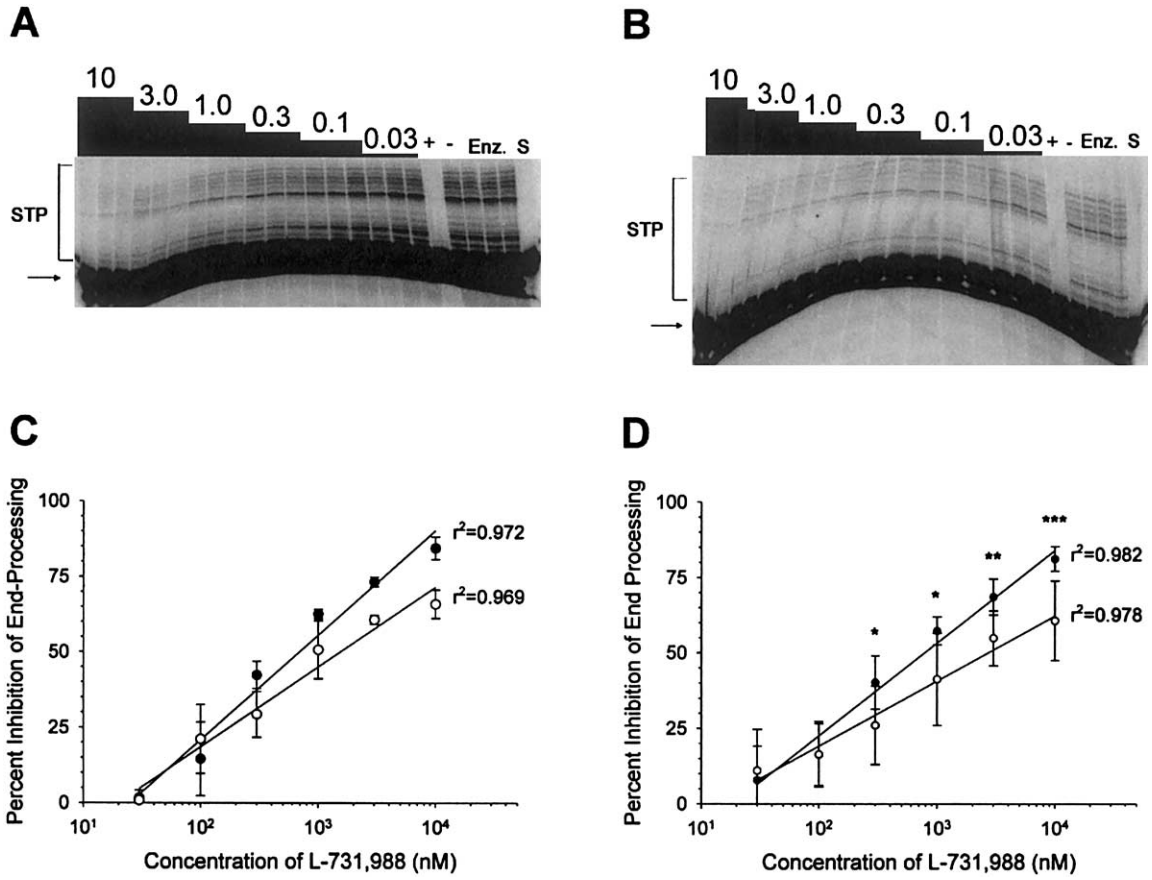

Fig. 10. IN_{G140S} is resistant to L-731,988. Panel A) 3′ end processing and strand transfer assays with the IN_{WT} protein. Panel B) 3′ end processing and strand transfer assays with IN_{G140S} protein. Concentrations of L-731,988, in μM, are given above each triplicate reaction. (+), 25 μM L-731,988: Lane 21 (−): 25 μM L-tartaric acid; (Enz.), substrate with IN; S = substrate with no enzyme; Reactions were performed using recombinant IN, V1/V2 substrate for 1 h at 37°C. Strand transfer products (STP) were separated from substrate (arrow) by denaturing SDS-PAGE. Both panels were incubated together on the PhosphorImager and the percent inhibition of strand transfer products, irrespective of enzyme activity, were calculated. Each image was adjusted at the same time to the same level; therefore, product intensities are directly comparable. This result is representative of three experiments. Panel C) quantification of the results from Panels A and B (one triplicate reaction). Panel D): the mean quantification for all nine replicates (three assays performed in triplicate) used to calculate the IC_{50}. P values were calculated at each point using student's unpaired t test assuming equal variances. $*P < 0.05$; $**P < 0.005$; $***P$, 0.0005. For Panels C and D: Closed circles are IN_{WT}, open circles are IN_{G140S}; each point is the mean; the error bars are one SD. Lines were generated using linear regression analysis; r^2 for each line are given on each graph.

Although disintegration activity has not been observed in vivo, mutations that affect disintegration activity also interfere with end processing and strand transfer activities of IN (Mazumder et al., 1994; van Gent, et al., 1992). Disintegration using the dumbbell substrate is also less likely to complicate steady-state kinetic analyses as only one complex, E + S, is likely to exist. Furthermore, only one product, rather than several, is formed. Finally, most compounds that inhibit disintegration in vitro also inhibit the 3′ end processing and strand transfer activities of IN in vitro (Farnet et al., 1998; Neamati et al., 1997; Neamati et al., 1998; Reddy et al., 1999; Robinson et al., 1996a; Robinson et al., 1996b). Thus, disintegration is a useful measure of IN activity and is the enzymatically-mediated reversal of the strand transfer reaction. The diketoacids are relatively selective inhibitors of strand transfer, rather than end processing or disintegration (Hazuda et al., 2000). It has been hypothesized that the diketoacids bind to the host DNA binding site, rather than to the viral DNA binding site (Hazuda et al., 2000). Our results on cross-resistance, coupled with previously published findings that L-CA blocks both catalysis and strand transfer (Robinson et al., 1996a; Robinson et al., 1996b), would suggest that L-CA may alter both the host DNA and viral DNA binding sites but not substrate binding affinity.

A strong correlation between attenuation of end processing and strand transfer and disintegration was observed for both IN_{WT} and IN_{G140S} (Figs. 6 and 7). Steady-state kinetic analyses using retroviral IN's have been performed previously (Chow and Brown, 1994b; Jones et al., 1992; Tramontano et al., 1998; Zhu et al., 1999); therefore, we reasoned that steady-state kinetic analysis could be used to better understand the effect of mutations on IN. Our results correlate well with steady state kinetic analyses of other IN proteins. A decrease in the velocity of the disintegration reaction catalyzed by IN_{G140S} (Fig. 8) was observed, sug-

gesting that the effect of the G140S mutation was at catalysis, rather than substrate binding, as similar concentrations of wild-type and mutant IN's bound virtually equal amounts of HIV LTR oligonucleotide DNA (Fig. 9). The steady-state kinetic results in combination with the LTR binding results suggest that similar levels of actively-folded protein were present for both wild-type and mutant IN, and that impaired catalysis of IN_{G140S} alone accounts for the defect in its enzymatic activities. However, we cannot rule out the possibility that the mutation affects IN multimerization or folding, which could affect catalysis without affecting DNA binding, or that these results might not be more profound at physiologically relevant low protein levels, since IN_{G140S} at the lowest protein concentrations demonstrated the most pronounced, yet statistically insignificant, effect on DNA binding. The level of attenuation observed for IN_{G140S} is consistent with that reported for disintegration activity mediated by the core catalytic domain of an IN_{G140A} mutant (Greenwald et al., 1999). Finally, the increase in formation of two LTR circles during replication of HIV containing this mutation (Fig. 3) is consistent with effects of the mutation on catalysis but not cellular entry, reverse transcription, or nuclear import of the viral genome. Abortive integration (Fig. 3) may be responsible for the delay in HIV replication seen in both MT-2 cells (Fig. 2) and H9 cells (King and Robinson, 1998), especially since the delay in MT-2 cells (Fig. 2) correlated with the maximum increase in two LTR circle DNA to cDNA ratio in H9 cells (Fig. 3).

The glycine at position 140 of HIV IN is phylogenetically conserved (Kulkosky et al., 1992). From the crystallographic structure of the catalytic core domain of HIV IN (Dyda et al., 1994; Goldgur et al., 1998; Maignan et al., 1998), this glycine appears to act as a crucial anchor residue. It is the final residue within an ordered β-sheet, β5, directly adjacent to a disordered loop domain, α4, amino acids 141 to 149. The importance of this residue as an anchor for the disordered loop was recently demonstrated through site-directed mutagenesis (Greenwald et al., 1999). Several structures suggest that G140 is an anchor for the β5–α4 junction and lies near the putative active site, adjacent to the region in which the divalent metal ion is complexed (Goldgur et al., 1998; Maignan et al., 1998). The small side chains of G140 and G149 of IN may allow the disordered loop to fold towards the face of the catalytic core domain and are postulated to aid in the coordination of divalent cation and formation of the active IN catalytic site (Greenwald et al., 1999). The cycling between active and inactive conformations that may involve movement of the disordered loop is proposed to be critical in the IN catalytic cycle (Asante-Appiah et al., 1998; Asante-Appiah and Skalka, 1997) and is supported by the crystallographic data: this region has high temperature factors (Greenwald et al., 1999), suggesting it is flexible (Goldgur et al., 1998; Maignan et al., 1998). Substitution of larger polar or non-polar side chains at the site of the molecular hinge may result in decreased ease of native conformational movements. In this manner, the IN_{G140S} may directly result in loss of catalytic activity of IN. The crystal structures of IN_{G140A}, IN_{G149A}, and the double mutant display subtle alterations in morphology, with increased rigidity in the disordered loop and altered enzymatic activity (Greenwald et al., 1999).

In accordance with the hinge model, the effects of mutation of either G140 or G149 should be limited to catalytic activities and should not involve protein stability or substrate binding. In support of this prediction, no disproportionate decreases in IN_{G140S} catalytic activity were observed at increased or decreased temperatures when compared to wild-type IN (not shown), suggesting that IN protein stability is not affected by this mutation. The catalytic core domain of IN has previously been shown to be important in the specific recognition of viral DNA near the conserved CpA dinucleotide (Shibagaki and Chow, 1997), while cross-linking studies have identified loop amino acids which make direct contacts with substrate DNA molecules (Heuer and Brown, 1998; Jenkins et al., 1997). However, no significant difference in HIV LTR binding between IN_{G140S} and IN_{WT} was observed (Fig. 9). These results are in agreement with steady-state kinetic analysis (Fig. 7) in which the V_{max} of IN_{G140S} is decreased with no change in the apparent affinity of this mutant for db-Y1 as measured by the K_m. Our observations combined with those of Greenwald et al., (1999) suggest that G140 has little effect on either specific recognition of viral DNA or target DNA binding.

Utilizing IC_{50} analyses we have demonstrated an approximately four-fold decrease in sensitivity of purified recombinant IN_{G140S} to L-CA and to L-731,988 when compared to wild-type IN (Table 1 and Fig. 10). Although this is a modest effect on inhibitor susceptibility observed in vitro, the direct effects of this mutation on inhibitor-susceptibility have been observed in vivo (King and Robinson, 1998) (Fig. 4). This resistance phenotype was limited to IN inhibitors (Fig. 5). Computer analysis of the crystal structure of an ASV IN:inhibitor complex (Lubkowski et al., 1998), with an analogous glycine to serine mutation modeled into the structure, suggests that this mutation would reduce the size of the drug binding pocket (King, P.J., Poulos, T., and Robinson, W.E., Jr. unpublished results). Thus, the mutation alone may occlude the binding of L-CA and L-731,988 by size alone. Our results suggest that IN_{G140S} is, at least in part, directly responsible for conferring IN inhibitor-resistance to mutant HIV. Similar attenuation of viral growth, enzyme function, and degree of inhibitor resistance were reported for HIV resistant to the diketoacids (Hazuda et al., 2000).

Recent data suggest that IN containing mutations at phenylalanine 185 (F185K), cysteine 280 (C280S), and glycine 140 (G140S) was no more resistant to L-CA than a protein containing just the F185K and C280S mutations (Pluymers et al., 2000). However, the IC_{50} of L-CA against IN containing the F185K and C280S mutations in the disintegration reaction was 2.0 μM, approximately 12-fold higher than reported by our laboratory and others (Farnet et al.,

1998; Robinson et al., 1996a; Robinson et al., 1996b; Zhu et al., 1999). Thus, the wild-type IN was more resistant to the effects of L-CA than the IN_{G140S} mutant IN. The mechanisms by which the F185K and/or C280S mutations confer resistance to L-CA should be further evaluated.

The G140S mutation confers cross-resistance to L-731,988. Furthermore, resistance mutations for L-731,988 (Hazuda et al., 2000) are similar to residues predicted to form the L-CA binding pocket (Robinson et al., 1996a; Sotriffer et al., 2000). More recently, Sotriffer et al. (2000) utilized computational docking to demonstrate that L-CA more completely fills an inhibitor-binding groove than do other IN inhibitors. Such docking experiments suggested that L-CA interacts with lysines 156 and 159, as well as cysteine 65, threonine 66, histidine 67, glutamine 148, and glutamate 152. The most favorable contacts are glutamate 152, a member of the catalytic triad, and glutamine 148 (Sotriffer et al., 2000). These results are quite similar to previously reported docking experiments utilizing a different crystal structure and an alternative docking program (Robinson et al., 1996a). To date the binding pocket for L-731,988 and other diketoacids has not been described. The cross-resistance data support the hypothesis that one drug binding pocket exists for dicaffeoylquinic acids, dicaffeoyltartaric acids, and diketoacids. Furthermore, position 140 of integrase is an important residue both for susceptibility of the protein to inhibition by several classes of inhibitor and for catalysis but conservation of the glycine residue is not absolutely required for viral replication or integration.

Materials and methods

Cells and virus

MT-2 cells are $CD4^+$ T-lymphoblastoid cells that are completely lysed by X4 isolates of HIV. HIV_{NL4-3} and HIV_{NL4-3} containing the G140S IN mutation ($HIV_{NL4-3:ING140S}$) were obtained as described (King and Robinson, 1998) (HIV_{NL4-3} GenBank #M19921; $HIV_{NL4-3:ING140S}$ GenBank #AF078150). Briefly, following selection under L-CA, the reference IN sequence was replaced by IN containing only the G140S substitution. Plasmids were subsequently transfected into HeLa cells, the cells were washed, and then cultured with H9 cells, a $CD4^+$ T-lymphoblastoid cell line that supports chronic infection by HIV. Virus was obtained when H9 cells became 100% positive for HIV antigens by IFA. Cells were grown in RPMI-1640 containing 25 mM 4-(2-hydroxyethyl)-1-piperazineethanesulfonic acid and supplemented with 11.5% fetal bovine serum (Gemini Biosciences) and 2 mM L-glutamine. All HIV were obtained from H9 cell culture supernatants clarified of cells by low speed centrifugation followed by filtration through 0.45 μm cellulose acetate filters.

Viral quantification

HIV was quantified using three separate assays. (1) RT activity. Virus-associated RT was measured as [^{3}H]dTTP incorporation into a poly(rA)-oligo(dT) template by a modification (Robinson et al., 1989) of a method described by Poeisz et al. (1980). (2) $TCID_{50}$. The numbers of infectious particles were determined by endpoint dilution analysis on MT-2 cells in replicates of eight. Endpoints were measured after 21 days (greater than seven replicative cycles). The $TCID_{50}$ represents one infectious particle per inoculum and is reported as the number of infectious particles per ml of culture fluid (Robinson et al., 1989). (3) IFA. The percent of cells expressing HIV antigens was enumerated using methanol:acetone-fixed cells incubated first with human polyclonal anti-HIV-1 pooled immunoglobulin fraction followed by fluoresceinated goat anti-human IgG as described (Robinson et al., 1989).

Susceptibility of molecular clones to anti-HIV agents

The resistance profile of $HIV_{NL4-3:ING140S}$ to L-CA has been described, previously (King and Robinson, 1998). $HIV_{NL4-3:ING140S}$, $HIV_{NL4-3:IN7-3}$ containing the silent cloning mutations and IN from HIV multiply-passaged in tissue culture (King and Robinson, 1998), and HIV_{NL4-3} were incubated in triplicate with increasing concentrations of zidovudine, dideoxycytidine, dideoxyinosine, nelfinavir, L-CA, or L-731,988 for one h at 37°C. Next, MT-2 cells were added and the cells harvested for HIV-induced cytopathic effect four days later (King et al., 1999; King and Robinson, 1998; Montefiori et al., 1988; Robinson et al., 1996a; Robinson et al., 1996b). Cells were reduced by 50% and re-fed without additional anti-HIV compound on day two.

Cell lysis and sample preparation for real-time PCR

At each time point 1.0×10^6 cells were lysed in 100 μl of a lysis solution composed of equal parts solution A (100 mM KCl, 10 mM Tris-HCl pH 8.3, 2.5 mM $MgCl_2$) and solution B (10 mM Tris-HCl pH 8.3, 2.5 mM $MgCl_2$, 1% Tween-20, 1% Nonidet P40 and 20 μg of proteinase K per 1.0×10^6 cells. Cells were lysed at 65°C for 1 h, followed by heat-inactivation of proteinase K at 95°C for 15 minutes (Kellogg and Kwok, 1990).

Real-time PCR and oligonucleotide primers:

Primers were: AA55: 5′-CTGCTAGAGATTTTCCACACTGAC-3′ (HIV-1_{LAI} anti-sense 635–612) M667: 5′-GGCTAACTAGGGAACCCACTG-3′ (HIV-1_{LAI} sense 496–516) M661: 5′-CCTGCGTCGAGAGAGCTCCTCTGG-3′ (HIV-1_{LAI} anti-sense 695–672) MH535: 5′-AA-

CTAGGGAACCCACTGCTTAAG-3′ (HIV-1_{LAI} sense 9683–9697) MH536: 5′-TCCACAGATCAAGGATATCT-TGTC-3′ (HIV-1_{LAI} anti-sense 58–21)

Real-time PCR was performed using the Cepheid Smart Cycler (Fisher Scientific, Tustin, CA). PCR conditions were: initial denaturation at 95°C for 150 s followed by 40 rounds of cycling at 95°C for 15 s, then 61°C for 30 s. Each PCR reaction contained 0.2 μM each of dATP, dCTP, dGTP and dTTP, 1.5 mM $MgCl_2$, 20 mM Tris-HCl pH 8.4, 50 mM KCl, 0.625 U *Taq* DNA polymerase (GIBCO-BRL), 0.2 μM of each primer, and 0.25× SYBR-I Green (Sigma-Aldrich or Molecular Probes) and 2 μl of cell lysate in a 25 μl reaction volume. Following amplification, melt curve analysis between 60°C to 95°C (0.2°C/s) was performed to determine the T_m of the amplified product. The T_m of each reaction was compared to control reactions. Products with incorrect T_m contain primer dimers and are below the sensitivity of real-time PCR. HIV-1 specific primers pairs were used to detect minus strand strong stop, AA55/M667 (Zack et al., 1990), complete cDNA, M661/M667 (Zack et al., 1990), and two LTR circle DNA, MH535/MH536 (Butler et al., 2001). For two LTR circle DNA, PCR conditions were as described previously (Reinke et al., 2002): initial denaturation at 95°C for 150 s., followed by 40 rounds of cycling at 95°C for 15 s., then 59°C for 30 s. Following amplification, melt curve analysis between 60°C and 95°C (0.2°C/s) was performed to determine the T_m of the amplified product. Each PCR reaction contained 0.2 μM of each dNTP, 1.5 mM $MgCl_2$, 20 mM Tris-HCl pH 8.4, 5 μg non-acetylated BSA, 0.15 M trehalose, 0.2% Tween-20, 0.625 U Taq DNA polymerase (GIBCO-BRL), 0.2 μM of each primer, MH535 and MH536 (Butler et al., 2001), and 0.25× SYBR-I Green and 2 μl of cell lysate in a 25 μl reaction volume. All results were calculated as infected cell equivalents from standard curves using 20,000 to 20 HIV_{LAI} chronically infected H9 cells diluted into the DNA from 20,000 uninfected H9 cells.

Viral replication

Equal amounts of HIV_{NL4-3} and $HIV_{NL4-3:ING140S}$ by RT (10,000 cpm) or $TCID_{50}$ (20,000) were used to infect 5×10^5 MT-2 cells in triplicate wells of a 24-well plate (Costar). After 24 h at 37°C, cells were removed, washed, and replated. Culture supernatant fluid was removed from each well every other day and virus quantitated by RT release. Half of the cells were removed every other day and assayed by IFA to determine the number of HIV antigen positive cells.

Purification of recombinant IN

IN sequences from HIV_{NL4-3} and $HIV_{NL4-3:ING140S}$ were amplified by PCR using oligonucleotide primers, then introduced into a pET-based, *Escherichia coli* expression vector, as described previously (King and Robinson, 1998; Vincent et al., 1993). Purification of amino terminus six His-IN fusion proteins by Ni^{2+} affinity column chromatography was performed as described (King et al., 1999). Protein purity was assessed by sodium dodecylsulfate-polyacrylamide gel electrophoresis (SDS–PAGE) followed by Coomassie R_{250} staining. Imidazole fractions chosen for enzymatic analysis contained peak protein concentrations migrating at approximately 32,000 Da, and were greater than 90% pure.

Molecular activity analysis

The activity of purified recombinant IN was measured in the disintegration reaction, using the db-Y1 "dumbbell" substrate (Chow and Brown, 1994a) and in the 3′ end processing reaction using the V1/V2 substrate as described (Chow, 1997). Briefly, 5 nM of substrate was added to reactions containing equal concentrations of reference (IN_{WT}) or mutant (IN_{G140S}) proteins. The reactions were allowed to proceed for 1 h at 37°C and then were stopped by the addition of ethylenediaminetetraacetic acid (EDTA) to a final concentration of 18 mM, and the reactions placed on ice. Oligonucleotides were resolved by 15% PAGE containing 7M urea. Gels were dried and quantitated by PhosphorImager analysis using ImageQuant Software.

Steady-state kinetic analysis

IN_{WT} (35 nM) or IN_{G140S} (229 nM) were utilized in the disintegration reaction in the presence of db-Y1 at 100, 175, 250, 325, 400, and 500 nM. Reaction progress was measured at 4, 8, and 12 minutes by removing a portion of the reaction mixture, adding EDTA to a final concentration of 18 mM, and placing the sample on ice. Reaction progress at each time point for each substrate concentration was quantitated by PhosphorImager analysis. Initial velocities for each substrate concentration were defined as the slope of the progress curve (mol product per minute per mol IN).

50% inhibitory concentration (IC_{50}) analysis

IC_{50} of L-CA against both IN_{WT} and IN_{G140S} in the disintegration reaction using the Y-oligomer substrate were performed with IN at equal molecular activities. IN_{WT} was present at 25 nM and IN_{G140S} present at 195 nM in these experiments. For IC_{50} analyses of L-731,988, 250 nM IN_{WT} and 200 nM IN_{G140S} were incubated with increasing concentrations of L-731,988 and 10 nM V1/V2 substrate. The amount of product formed at increasing L-CA concentrations in the disintegration reaction or increasing L-731,988 concentrations in the strand transfer reaction over 1 h at 37°C were determined by PhosphorImager analysis following 15% denaturing PAGE.

Temperature-dependence and divalent metal ion usage

The disintegration reaction using purified recombinant IN_{WT} (35 nM) and IN_{G140S} (230 nM) was performed with db-Y1 at increasing temperatures (20, 24, 27, 30, 37, 42, and 50°C), or at 37°C in the presence of 1, 2.5, 5, 10, 15, 20, and 40 mM $MnCl_2$, or 2.5, 5, 10, 15, 20, and 40 mM $MgCl_2$ or $ZnCl_2$. The amount of disintegration product formed by each enzyme under each condition in 1 h was determined by PhosphorImager analysis following 15% denaturing PAGE.

DNA-binding assay

Equal concentrations of IN_{WT} and IN_{G140S} or HEL were incubated with ^{32}P end-labeled 3′ end processing substrate (V1/V2) and DNA binding was assessed by binding to nitrocellulose filters as described (Chow, 1997). Bound DNA was measured by liquid scintillation counting (Scinti-Verse II, Fisher Scientific). Background binding of substrate by HEL at each concentration was subtracted.

PhosphorImager analysis

Dried denaturing polyacrylamide gels were exposed on a phosphor screen (Molecular Dynamics). Gels were removed and the screens scanned on a Molecular Dynamics Storm PhosphorImager. Quantification was performed using Molecular Dynamics ImageQuant. Gels were exposed for times that gave peak PhosphorImager units within the linear range of the phosphor screen (<100,000 units).

Acknowledgments

The HIV_{NL4-3} plasmid was obtained from the NIH AIDS Research and Reference Reagent Repository. Professor Manfred G. Reinecke at Texas Christian University kindly provided L-CA and L-731,988. The IN expression vector was a gift from Professor Samson Chow of the University of California in Los Angeles. The authors are indebted to Brenda R. McDougall for expert technical assistance. The authors also thank Professors Suzanne Sandmeyer, Hung Fan, and Marian Waterman for thoughtful comments on experimental design. This work was supported in part by grants from the Public Health Service: 5R01-AI41360 (WER), 5T32-GM07311 (PJK), 5T32-GM08620 (DLJ), and 5T32-AI07319 (RAR), the Burroughs-Wellcome Fund (99-2609, WER), and a Systemwide grant for biotechnology training from the University of California (JGV). WER is a Recipient of the Burroughs-Wellcome Fund Clinical Scientist Award in Translational Research.

References

Andrake, M.D., Skalka, A.M., 1996. Retroviral integrase, putting the pieces together. J. Biol. Chem. 271, 19633–19636.

Asante-Appiah, E., Seeholzer, S., Skalka, A., 1998. Structural determinants of metal-induced conformational changes in HIV-1 integrase. J. Biol. Chem. 273, 35078–35087.

Asante-Appiah, E., Skalka, A.M., 1997. A metal-induced conformational change and activation of HIV-1 integrase. J. Biol. Chem. 272.

Brown, P.O., 1997. Integration, in: Coffin, J.M., Hughes, S.H., Varmus, H.E. (Eds.), Retroviruses, 1 ed. Cold Spring Harbor Laboratory Press, Plainview, NY, pp. 161–203.

Brown, P.O., Bowerman, B., Varmus, H.E., Bishop, J.M., 1989. Retroviral integration: structure of the initial covalent product and its precursor, and a role for the viral IN protein. Proc. Natl. Acad. Sci. USA 86, 2525–2529.

Bujacz, G., Alexandratos, J., Zhou-Liu, Q., Clement-Mella, C., Wlodawer, A., 1996a. The catalytic domain of human immunodeficiency virus integrase: ordered active site in the F185H mutant. FEBS Letters 398, 175–178.

Bujacz, G., Jaskolski, M., Alexandratos, J., Wlodawer, A., Merkel, G.M., Katz, R.A., Skalka, A.M., 1996b. The catalytic domain of avian sarcoma virus integrase: conformation of the active-site residues in the presence of cations. Structure 4, 89–96.

Bushman, F.D., Craigie, R., 1991. Activities of human immunodeficiency virus (HIV) integration protein in vitro: specific cleavage and integration of HIV DNA. Proc. Natl. Acad. Sci., USA 88, 1339–1343.

Butler, S.L., Hansen, M.S.T., Bushman, F.D., 2001. A quantitative assay for HIV DNA integration in vivo. Nature Med. 7, 631–634.

Chow, S.A., 1997. In vitro assays for activities of retroviral integrase. Methods. A Companion to Methods in Enzymology 12, 306–317.

Chow, S.A., Brown, P.O., 1994a. Juxtaposition of two viral DNA ends in a bimolecular disintegration reaction mediated by multimers of human immunodeficiency virus type 1 or murine leukemia virus integrase. J. Virol. 68, 7869–7878.

Chow, S.A., Brown, P.O., 1994b. Substrate features important for recognition and catalysis by human immunodeficiency virus type 1 integrase identified by using novel DNA substrates. J. Virol. 68, 3896–3907.

Chow, S.A., Vincent, K.A., Ellison, V., Brown, P.O., 1992. Reversal of integration and DNA splicing mediated by integrase of human immunodeficiency virus. Science 255, 723–726.

Dyda, F., Hickman, A.B., Jenkins, T.M., Engelman, A., Craigie, R., Davies, D.R., 1994. Crystal structure of the catalytic domain of HIV-1 integrase: similarity to other polynucleotidyl transferases. Science 266, 1981–1986.

Engelman, A., Craigie, R., 1992. Identification of conserved amino acid residues critical for human immunodeficiency virus type 1 integrase function in vitro. J. Virol. 66, 6361–6369.

Engelman, A., Liu, Y., Chen, H., Farzan, M., Dyda, F., 1997. Structure-based mutagenesis of the catalytic domain of human immunodeficiency virus type 1 integrase. J. Virol. 71, 3507–3514.

Espeseth, A.S., Felock, P., Wolfe, A., Witmer, M., Grobler, J., Anthony, N., Egbertson, M., Melamed, J.Y., Young, S., Hamill, T., Cole, J.L., Hazuda, D.J., 2000. HIV-1 integrase inhibitors that compete with the target DNA substrate define a unique strand transfer conformation for integrase. Proc. Natl. Acad. Sci. USA 97, 11244–11249.

Farnet, C.M., Wang, B., Hansen, M., Lipford, J.R., Zalkow, L., Robinson, W.E., Jr., Siegel, J., Bushman, F., 1998. Human immunodeficiency virus type 1 cDNA integration: new aromatic hydroxylated inhibitors and studies of the inhibition mechanism. Antimicrob. Agents Chemother. 42, 2245–2253.

Fujiwara, T., Mizuuchi, K., 1988. Retroviral DNA integration: structure of an integration intermediate. Cell 54, 497–504.

Goldgur, Y., Craigie, R., Cohen, G.H., Fujiwara, T., Tomokazu, Y., Fujishita, T., Sugimoto, H., Endo, T., Murai, H., Davies, D.R., 1999. Structure of the HIV-1 integrase catalytic domain complexed with an

inhibitor: a platform for antiviral drug design. Proc. Natl. Acad. Sci. USA 96, 13040–13043.

Goldgur, Y., Dyda, F., Hickman, A.B., Jenkins, T.M., Craigie, R., Davies, D.R., 1998. Three new structures of the core domain of HIV-1 integrase: an active site that binds magnesium. Proc. Natl. Acad. Sci. USA 95, 9150–9154.

Greenwald, J., Le, V., Butler, S.L., Bushman, F.D., Choe, S., 1999. The mobility of an HIV-1 integrase active site loop is correlated with catalytic activity. Biochemistry 38, 8892–8898.

Hazuda, D.J., Pelock, P., Witmer, M., Wolfe, A., Stillmock, K., Grobler, J.A., Espeseth, A., Gabryelski, L., Schleif, W., Blau, C., Miller, M.D., 2000. Inhibitors of strand transfer that prevent integration and inhibit HIV-1 replication in cells. Science 287, 646–650.

Heuer, T., Brown, P., 1998. Photo-cross linking studies suggest a model for the architecture of an active human immunodeficiency virus type 1 integrase–DNA complex. Biochemistry 37, 6667–6678.

Jenkins, T.M., Esposito, D., Engelman, A., Craigie, R., 1997. Critical contacts between HIV-1 integrase and viral DNA identified by structure-based analysis and photo-crosslinking. EMBO J. 16, 6849–6859.

Johnson, M.S., McClure, M.A., Feng, D.-F., Gray, J., Doolittle, R.F., 1986. Computer analysis of retroviral *pol* genes: assignment of enzymatic functions to specific sequences and homologies with nonviral enzymes. Proc. Natl. Acad. Sci. USA 83, 7648–7652.

Jones, K.S., Coleman, J., Merkel, G.W., Laue, T.M., Skalka, A.M., 1992. Retroviral integrase functions as a multimer and can turn over catalytically. J. Biol. Chem. 267, 16037–16040.

Kellogg, D.E., Kwok, S., 1990. Detection of human immunodeficiency virus, in: Innis, M.A., Gelfand, D.H., Sninsky, J.J., White, T.J. (Eds.), PCR Protocols: a guide to methods and applications. Academic Press, Inc., San Diego, pp. 337–347.

King, P.J., Ma, G., Miao, W., Jia, Q., McDougall, B.R., Reinecke, M.G., Cornell, C., Kuan, J., Kim, T.R., Robinson, Jr., W.E., 1999. Structure-activity relationships: analogues of the dicaffeoylquinic and dicaffeoyltartaric acids as potent inhibitors of human immunodeficiency virus type 1 integrase and replication. J. Med. Chem. 42, 497–509.

King, P.J., Robinson, Jr., W.E., 1998. Resistance to the anti-human immunodeficiency virus type 1 compound L-chicoric acid results from a single mutation at amino acid 140 of integrase. J. Virol. 72, 8420–8424.

Kulkosky, J., Jones, K.S., Katz, R.A., Mack, J.P.G., Skalka, A.M., 1992. Residues critical for retroviral integrative recombination in a region that is highly conserved among retroviral/retrotransposon integrases and bacterial insertion sequence transposases. Mol. Cell. Biol. 12, 2331–2338.

LaFemina, R.L., Schneider, C.L., Robbins, H.L., Callahan, P.L., LeGrow, K., Roth, E., Schleif, W.A., Emini, E.A., 1992. Requirement of active human immunodeficiency virus type 1 integrase enzyme for productive infection of human T-lymphoid cells. J. Virol. 66, 7414–7419.

Leavitt, A.D., Shiue, L., Varmus, H.E., 1993. Site-directed mutagenesis of HIV-1 integrase demonstrates differential effects on integrase functions in vitro. J. Biol. Chem. 268, 2113–2119.

Lubkowski, J., Yang, F., Alexandratos, J., Wlodawer, A., Zhao, H., Burke, T.R., Jr., Neamati, N., Pommier, Y., Merkel, G., Skalka, A.M., 1998. Structure of the catalytic domain of avian sarcoma virus integrase with a bound HIV-1 integrase-targeted inhibitor. Proc. Natl. Acad. Sci. USA 95, 4831–4836.

Maignan, S., Guilloteau, J.-P., Zhou-Liu, Q., Clement-Mella, C., Mikol, V., 1998. Crystal structures of the catalytic domain of HIV-1 integrase free and complexed with metal cofactor: high level of similarity of the active site with other viral integrases. J. Mol. Biol. 282, 359–368.

Mazumder, A., Engelman, A., Craigie, R., Fesen, M., Pommier, Y., 1994. Intermolecular disintegration and intramolecular strand transfer activities of wild-type and mutant HIV-1 integrase. Nucleic Acids Res. 22, 1037–1043.

McDougall, B., King, P.J., Wu, B.W., Hostomsky, Z., Reinecke, M.G., Robinson, W.E., Jr., 1998. Dicaffeoylquinic and dicaffeoyltartaric acids are selective inhibitors of human immunodeficiency virus type 1 integrase. Antimicrob. Agents Chemother. 42, 140–146.

Miller, M.D., Wang, B., Bushman, F.D., 1995. Human immunodeficiency virus type 1 preintegration complexes containing discontinuous plus strands are competent to integrate in vitro. J. Virol. 69, 3938–3944.

Montefiori, D.C., Robinson, W.E., Jr., Schuffman, S.S., Mitchell, W.M., 1988. Evaluation of antiviral drugs and neutralizing antibodies against human immunodeficiency virus by a rapid and sensitive microtiter infection assay. J. Clin. Microbiol. 26, 231–235.

Neamati, N., Hong, H., Sunder, S., Milne, G.W., Pommier, Y., 1997. Potent inhibitors of human immunodeficiency virus type 1 integrase: identification of a four-point pharmacophore and tetracyclines as novel inhibitors. Mol. Pharmacol. 52, 1041–1055.

Neamati, N., Mazumder, A., Sunder, S., Owen, J.M., Tandon, M., Lown, J.W., Pommier, Y., 1998. Highly potent synthetic polyamides, bisdistamycins, and lexitropsins as inhibitors of human immunodeficiency virus type 1 integrase. Mol. Pharmacol. 54, 280–290.

Pluymers, W., Neamati, N., Pannecouque, C., Fikkert, V., Marchand, C., Burke, T.R., Jr., Pommier, Y., Schols, D., De Clercq, E., Debyser, Z., Witvrouw, M., 2000. Viral entry as the primary target for the anti-HIV activity of chicoric acid and its tetra-acetyl esters. Mol. Pharmacol. 58, 641–648.

Poiesz, B.J., Ruscetti, F.W., Gazder, A.F., Bunn, B.A., Minna, J.D., Gallo, R.C., 1980. Detection and isolation of type C retrovirus particles from fresh and cultured lymphocytes of a patient with cutaneous T-cell lymphoma. Proc. Natl. Acad. Sci. USA 77, 7415–7419.

Pommier, Y., Neamati, N., 1999. Inhibitors of human immunodeficiency virus integrase. Adv. Virus Res. 52, 427–458.

Reddy, M.R.R., Rao, M.R., Rhodes, D., Hansen, M.S.T., Rubins, K., Bushman, F.D., Venkateswarlu, Y., Faulkner, D.J., 1999. Lamellarin a 20-sulfate, an inhibitor of HIV-1 integrase active against HIV-1 virus in cell culture. J. Med. Chem. 42, 1901–1907.

Reinke, R.A., King, P.J., Victoria, J.G., McDougall, B.R., Ma, G., Mao, Y., Reinecke, M.G., Robinson, W.E., Jr., 2002. Dicaffeoyltartaric acid analogues inhibit human immunodeficiency virus type 1 (HIV-1) integrase and HIV-1 replication at non-toxic concentrations. J. Med. Chem. 45, 3669–3683.

Rice, P., Craigie, R., Davies, D., 1996. Retroviral integrases and their cousins. Curr. Opin. Struct. Biol. 6, 76–83.

Robinson, W.E., Jr., 1998. HIV integrase: the next target. Infect. Med. 15, 129–137.

Robinson, W.E., Jr., Cordeiro, M., Abdel-Malek, S., Jia, Q., Chow, S.A., Reinecke, M.G., Mitchell, W.M., 1996a. Dicaffeoylquinic acid inhibitors of human immunodeficiency virus integrase: inhibition of the core catalytic domain of human immunodeficiency virus integrase. Mol. Pharmacol. 50, 846–855.

Robinson, Jr., W.E., Montefiori, D.C., Gillespie, D.H., Mitchell, W.M., 1989. Complement-mediated, antibody-dependent enhancement of HIV-1 infection in vitro is characterized by increased protein and RNA syntheses and infectious virus release. J. Acquir. Immune Defic. Syndr. 2, 33–42.

Robinson, W.E., Jr., Reinecke, M.G., Abdel-Malek, S., Jia, Q., Chow, S.A., 1996b. Inhibitors of HIV-1 replication that inhibit HIV integrase. Proc. Natl. Acad. Sci. USA 93, 6326–6331.

Roth, M., Schwartzberg, P., Goff, S., 1989. Structure of the termini of DNA intermediates in the integration of retroviral DNA: dependence on IN function and terminal DNA sequence. Cell 58, 47–54.

Sakai, H., Kawamura, M., Sakuragi, J., Sakuragi, S., Shibata, R., Ishimoto, A., Ono, N., Ueda, S., Adachi, A., 1993. Integration is essential for efficient gene expression of human immunodeficiency virus type 1. J. Virol. 67, 1169–74.

Sherman, P.A., Dickson, M.L., Fyfe, J.A., 1992. Human immunodeficiency virus type 1 integration protein: DNA sequence requirements for cleaving and joining reactions. J. Virol. 66, 3593–3601.

Sherman, P.A., Fyfe, J.A., 1990. Human immunodeficiency virus integration protein expressed in Escherichia coli possesses selective DNA cleaving activity. Proc. Natl. Acad. Sci. USA 87, 5119–5123.

Shibagaki, Y., Chow, S.A., 1997. Central core domain of retroviral integrase is responsible for target site selection. J. Biol. Chem. 272, 8361–8369.

Sotriffer, C.A., Ni, H., McCammon, A., 2000. Active site binding modes of HIV-1 integrase inhibitors. J. Med. Chem. 43, 4109–4117.

Stevenson, M., Haggerty, S., Lamonica, C.A., Meier, C.M., Welch, S.K., Wasiak, A.J., 1990. Integration is not necessary for expression of human immunodeficiency virus type 1 protein products. J. Virol. 64, 2421–5.

Taddeo, B., Haseltine, W.A., Farnet, C.M., 1994. Integrase mutants of human immunodeficiency virus type 1 with a specific defect in integration. J. Virol. 68, 8401–8405.

Tramontano, E., Colla, P., Cheng, Y., 1998. Biochemical characterization of the HIV-1 integrase 3′-processing activity and its inhibition by phosphorothioate oligonucleotides. Biochemistry 37, 7237–7243.

van Gent, D.C., Groeneger, A.A., Plasterk, R.H., 1992. Mutational analysis of the integrase protein of human immunodeficiency virus type 2. Proc. Natl. Acad. Sci. USA 89, 9598–9602.

Vincent, K.A., Ellison, V., Chow, S.A., Brown, P.O., 1993. Characterization of human immunodeficiency virus type 1 integrase expressed in Escherichia coli and analysis of variants with amino-terminal mutations. J. Virol. 67, 425–437.

Wiskerchen, M., Muesing, M.A., 1995. Human immunodeficiency virus type 1 integrase: effects of mutations on viral ability to integrate, direct viral gene expression from unintegrated viral DNA templates, and sustain viral propagation in primary cells. J. Virol. 69, 376–386.

Zack, J.A., Arrigo, S.J., Weitsman, S.R., Go, A.S., Haislip, A., Chen, I.S.Y., 1990. HIV-1 entry into quiescent primary lymphocytes: molecular analysis reveals a labile, latent viral structure. Cell 61, 213–222.

Zhu, K., Cordeiro, M.L., Atienza, J., Robinson, Jr., W.E., Chow, S.A., 1999. Irreversible inhibition of human immunodeficiency virus type 1 integrase by dicaffeoylquinic acids. J. Virol. 73, 3309–3316.